

# The G-CLEF Spectrograph Optical Design

Gábor Fűrész<sup>a</sup>, Harland Epps<sup>b</sup>, Stuart Barnes<sup>c</sup>, William Podgorski<sup>a</sup>, Andrew Szentgyorgyi<sup>a</sup>, Mark Mueller<sup>a</sup>, Daniel Baldwin<sup>a</sup>, Jacob Bean<sup>d</sup>, Henry Bergner<sup>a</sup>, Moo-Yung Chun<sup>g</sup>, Jeffrey Crane<sup>e</sup>, Janet Evans<sup>a</sup>, Ian Evans<sup>a</sup>, Jeff Foster<sup>a</sup>, Thomas Gauron<sup>a</sup>, Dani Guzman<sup>f</sup>, Edward Hertz<sup>a</sup>, Andres Jordán<sup>f</sup>, Kang-Min Kim<sup>g</sup>, Kenneth McCracken<sup>a</sup>, Timothy Norton<sup>a</sup>, Mark Ordway<sup>a</sup>, Chan Park<sup>g</sup>, Sang Park<sup>a</sup>, Dave Plummer<sup>a</sup>, Alan Uomoto<sup>e</sup>, In-Soo Yuk<sup>g</sup>

<sup>a</sup>Harvard-Smithsonian Center for Astrophysics, 60 Garden St., Cambridge, MA 02140;

<sup>b</sup>UCO/Lick Observatory, University of California, Santa Cruz, CA 95064;

<sup>c</sup>Stuart Barnes Optical Design, Sumatrastraat 108a 1094NK Amsterdam, The Netherlands;

<sup>d</sup>University of Chicago, 640 S. Ellis Ave, Chicago, IL 60637;

<sup>e</sup>The Observatories of the Carnegie Institution for Science, 813 Santa Barbara St., Pasadena, CA 91101;

<sup>f</sup>Pontificia Universidad Católica de Chile, Vicuna Mackenna 4860, Macul, Santiago, Chile;

<sup>g</sup>Korea Astronomy and Space Science Institute (KASI), 776 Daedeokdae-ro, Yuseong-gu, Daejeon, Republic of Korea;

## ABSTRACT

The GMT-Consortium Large Earth Finder (G-CLEF) is a fiber fed, optical echelle spectrograph, which has been selected as a first light instrument for the Giant Magellan Telescope (GMT) currently under construction at the Las Campanas Observatory. We designed G-CLEF as a general-purpose echelle spectrograph with a precision radial velocity (PRV) capability goal of 0.1 m/s, which will enable it to detect/measure the mass of an Earth-sized planet orbiting a Solar-type star in its habitable zone. This goal imposes challenging requirements on all aspects of the instrument and some of those are best incorporated directly into the optical design process. In this paper we describe the preliminary optical design of the G-CLEF instrument and briefly describe some novel solutions we have introduced into the asymmetric white pupil echelle configuration.

**Keywords:** Echelle spectrograph, white pupil, optical design, Mangin mirror, precision radial velocity, G-CLEF, GMT

## 1. INTRODUCTION – THE INITIAL DESIGN CONSTRAINTS AND CONSIDERATIONS

The GMT-Consortium Large Earth Finder (G-CLEF<sup>1</sup>) is a general-purpose, fiber fed echelle spectrograph being built for the 25.4m Giant Magellan Telescope (GMT<sup>2</sup>) by a consortium of institutions led by the Harvard-Smithsonian Center for Astrophysics (CfA) and consisting of the Carnegie Observatories, Pontificia Universidad Católica de Chile, the Korean Astronomy and Space Science Institute and the University of Chicago. The G-CLEF Science Working Group developed the science case for G-CLEF, which was used to further develop the driving requirements for the instrument. The design was developed to meet and comply with these guidelines.

As a general use instrument, G-CLEF was required to provide a 3500Å-1μm wavelength coverage and also enable multiple spectral resolutions up to at least R=100,000, to enable a wide range of science cases. Since one of the leading applications is exoplanet research, G-CLEF was designed to have a precision radial velocity (PRV) capability. For this reason, we adopted the white pupil optical layout<sup>3</sup> as it has proven to be an important ingredient in achieving <1 m/s precision, and thus enabling the study of low mass exoplanets. Several successful existing and planned instruments (e.g. HARPS, ESPRESSO, etc.) employ this design approach, which not only minimizes the size of camera optics, but more importantly for PRV applications, provides a relatively uniform pupil illumination of the spectrograph camera at each wavelength over a wide bandpass. We also adopted the use of two separate collimators with different focal lengths, the asymmetric white pupil arrangement<sup>4</sup> that enables to further decrease the size of the camera optics. Although this comes at a price of increasing the ray angles within the camera, the sheer size of G-CLEF required us to reduce camera lens diameters. Since the size of the camera lenses is moderate, we could use the full range of optical glasses that are currently produced, and we also could keep the cost of materials and fabrication lower.

To reach the required 100k resolution on a 25.4m telescope we chose an R4 echelle and the largest available commercial grating format (by Richardson Grating Laboratory). This set the collimated beam size at 300mm and required a 3x1 mosaic grating. We determined the focal length of the pupil transfer (secondary collimator) mirror by a trade study, which concluded that a 3:2 compression ratio was optimal. This set the beam diameter 200mm at the camera. At this size all glasses from the full Ohara i-line catalog are obtainable at affordable prices, while the field angles also remain below a manageable 7.5 degrees. To cover the wide spectral passband of 3500Å-1μm at high resolution and allow for simultaneous recording of an object and sky spectra, we decided to split the wavelength coverage between a blue and a red arm with a dichroic. Each camera arm utilizes the largest currently available detector format (90x90mm).

The PRV operation requires highly stable slit illumination, gravity invariant deployment, as well as a pressure and temperature controlled environment. For further details see the papers in this proceedings describing the systems engineering error budget for G-CLEF<sup>5</sup> and the opto-mechanical design<sup>6</sup>. To meet the PRV goals we decided to use a fiber feed, even though this choice reduced throughput at the blue end of our passband, due to decreased internal transmission of the optical fiber. However, executing another trade study, we investigated the possibilities of using an optical relay system and shortening the fiber length. As a result we arrived at a hybrid solution that puts the fiber feed on the telescope but at a relayed focal plane, near the edge of the telescope mount, therefore decreasing the fiber length to approximately 15 meters. This is very short, given the size of the telescope, that there is no Nasmyth platform, and considering the requirement for a gravity invariant location of the instrument. Our approach for the PRV-minded fiber link is described by another paper in these proceedings<sup>7</sup>. G-CLEF has several different fiber feeds to provide a number of different resolutions and throughputs, according to the requirements of science programs discussed in the science case (see Section 2.3).

The design philosophy and the process of getting to the final, optimized spectrograph configuration given below, is described elsewhere<sup>8</sup>. That publication also explains how we came to use a cylindrical Mangin mirror for correction of field curvature, and the benefits of the improved access to the white pupil zone, as well as other novel optimization aspects of how the design provides a highly uniform and stable PSF that is key for PRV measurements.

## 2. G-CLEF OPTICAL DESIGN

### 2.1 Final Design Parameters and Layout

The preliminary design (PDR) baseline G-CLEF optical layout is shown on Figure 1. The light enters from the optical fibers at f/3 focal ratio, tilted by 7.5 degrees with respect to the optical axis of the parabolic collimator mirror, M1. A cemented doublet in front of the fiber input converts the focal ratio to f/8 (see Figure 2) and produces a virtual slit. This virtual image of the fiber end is located at the focus of the collimator, 2400mm away from the surface vertex point.

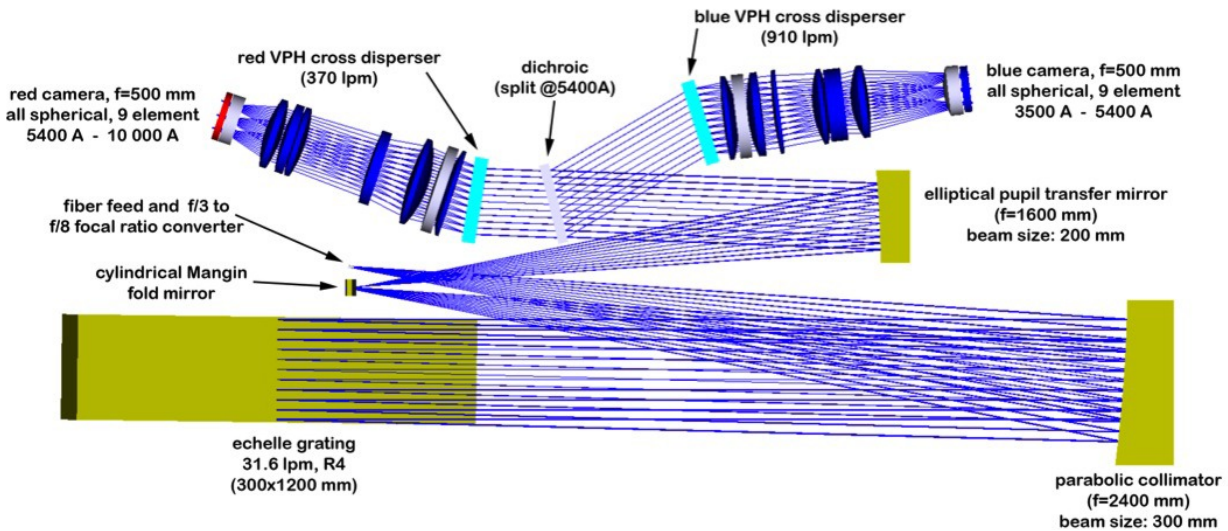


Figure 1 Optical layout of the G-CLEF spectrograph The components shown would fit on a 3.5m x 1.2m footprint optical table. The main dispersion is in and out of the plane of the figure. The given values correspond to the final design.

The focal ratio conversion optics allows for multiple fibers to be placed along a short, 1mm long pseudo-slit. Such field size is sufficient to accommodate multiple fibers (such as the 7 fibers of the pupil sliced PRV mode, and an additional sky fiber) of a given operational mode. See more on the different spectrograph operational modes in Section 2.3.

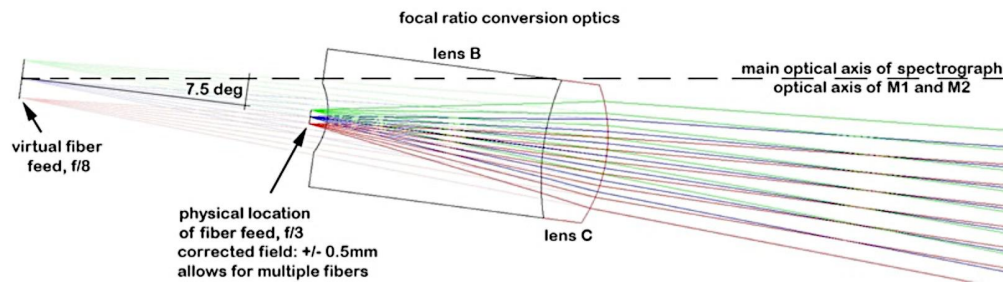


Figure 2 Close-up view of the fiber feed and focal ratio conversion optics

Element	Radius of curv. [mm]	Thickness [mm]	Material	Diameter [mm]
LB front	-4.000	12.552	PBM8Y	2
LB back/LC front	14.902	3.682	BAL15Y	4
LC back	-8.951			4
to virtual focus		-33.997		

Table 1 Prescription of the focal ratio conversion optics

The collimated beam has a diameter of 300mm, and illuminates an R4 echelle grating that is 300x1200mm, with 31.6 line/mm ruling density. The location of the grating mid-plane is just behind the slit, 2600mm away from the collimator vertex. The grating face is tilted at 75.6°. The true Littrow condition is slightly compromised by a 0.75°  $\gamma$  angle, a small clockwise rotation of the grating in the plane of Figure 1. Therefore the dispersed beam hits the collimator in second-pass over an elongated area, a bit farther away from the optical axis with respect to the circular first-pass polychromatic footprint of the incoming beam.

The refocused, monochromatic beams clear the fiber slit by converging to a point in-between the fiber input and the grating, due to the introduction of the small  $\gamma$  angle of the echelle. A Mangin fold mirror intercepts the converging light rays before arriving at an intermediate focus point and sends them towards a secondary collimator, the pupil transfer mirror. This Mangin mirror has cylindrical surfaces on its front and back, and serves as the field flattener of the system. An isometric and cross sectional view of the Mangin mirror is given in Figure 3, along with the optical prescription in Table 2. The Mangin mirror is asymmetric along the dispersion axis, since the longer wavelength end of an echelle order extends farther away from the optical axis. This is apparent as the edge thickness of the mirror at the left is more than at the right. While the beam footprint sizes are relatively small on the Mangin mirror, we all kept those over 1 mm by design enforcing a 40mm minimum distance from the first pass on the front of the fold mirror to the intermediate focus.

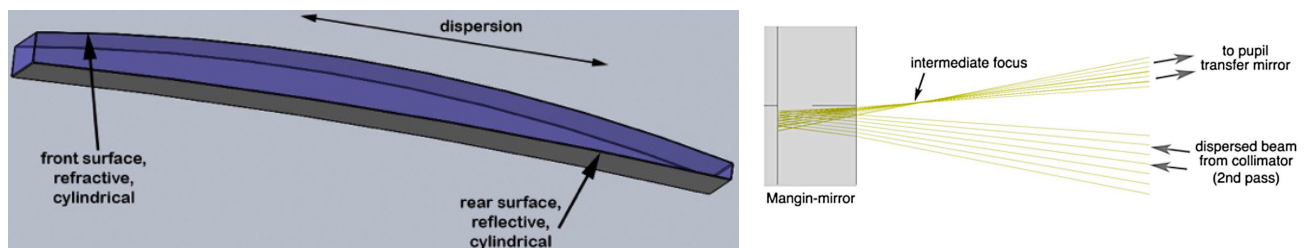


Figure 3 Isometric and cross sectional view of the Mangin fold mirror

Element	Radius of curv. [mm]	Thickness [mm]	Material	Diameter [mm]
Mangin front, 1 <sup>st</sup> pass	-1049.483	12.552	FUSED SILICA	25
Mangin rear	-3232.464	3.682	mirror	
Mangin front, 2 <sup>nd</sup> pass	-1049.483		FUSED SILICA	25

Table 2 Optical prescription of the Mangin fold mirror

The next optical element is the pupil transfer mirror, which has a focal length of 1600 mm, or 2/3 of the main collimator. This mirror has a conic constant of -0.88305, and thus is a prolate ellipsoid. The optical axis of the pupil transfer mirror is coincident with that of the main collimator.

Due to the decreased focal length of the pupil transfer mirror with respect to the main collimator, the re-collimated beam has a diameter of 200mm and therefore allows to use a smaller dichroic, cross disperser and camera optics. The geometry of the overall spectrograph layout allows greater access to the white pupil zone, which is conjugate to the echelle grating surface<sup>8</sup>. We chose to put the dichroic before the white pupil, so the cross disperser and a large portion of the camera lenses can be located within the white pupil zone. This is to minimize optical aberrations and achieve more uniform PSF across the echellogram<sup>8</sup>. The dichroic substrate is 30mm thick and made of fused silica, with an aperture of 250x370mm. The dichroic is tilted at 14 degrees respect to the common optical axis of the collimator and the pupil transfer mirror.

The cross dispersers are VPH gratings, sandwiched between two 20mm thick fused silica, plane-parallel glass plates. The blue cross disperser has a groove density of 910 lines/mm, while the red VPH has a 370 lines/mm groove density. The blue cross disperser is 450mm away from the dichroic, in order to clear the collimated beam between the pupil transfer mirror and the dichroic, since the blue arm is folded to minimize overall instrument footprint. The red cross disperser is only 200mm away from the dichroic, since there is no constraint (from the spectrograph main frame) on the location of the red arm.

## 2.2 Camera Design

Both cameras are based on the Keck Cosmic Web Imager<sup>9</sup> camera design, and employ 9 elements of Ohara i-line glasses and calcium fluoride. All lenses are spherical to minimize risk and cost, as well as to allow for more forgiving tolerancing in manufacturing and for mounting/alignment. We also developed alternative camera designs employing fewer elements, but aspheric surfaces, similar to the ESPRESSO designs<sup>10</sup>. However, a detailed performance analysis<sup>8</sup> showed that our goals of spatially highly uniform and stable PSF can be better met using the 9-element all-spherical design. For details refer to [8].

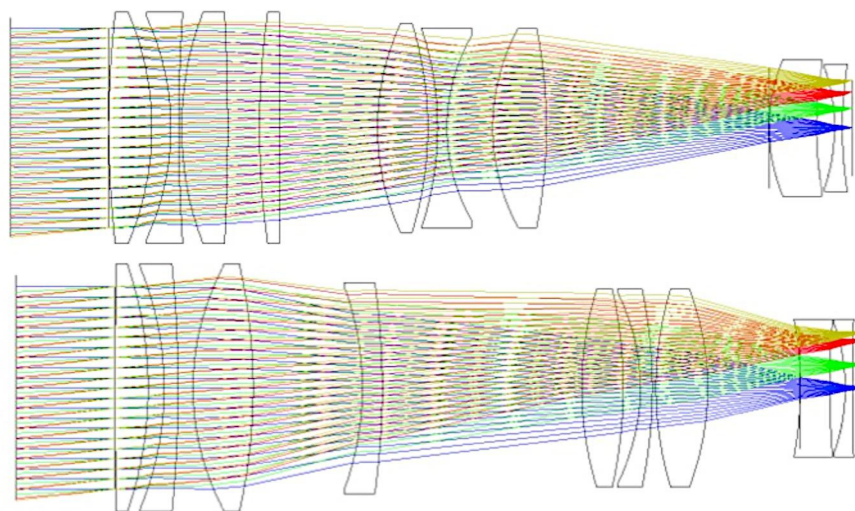


Figure 4 Layout of the blue (top) and red (bottom) camera optics. Lens L1 is on the left, L9 is at far right. See Table 3 and 4.

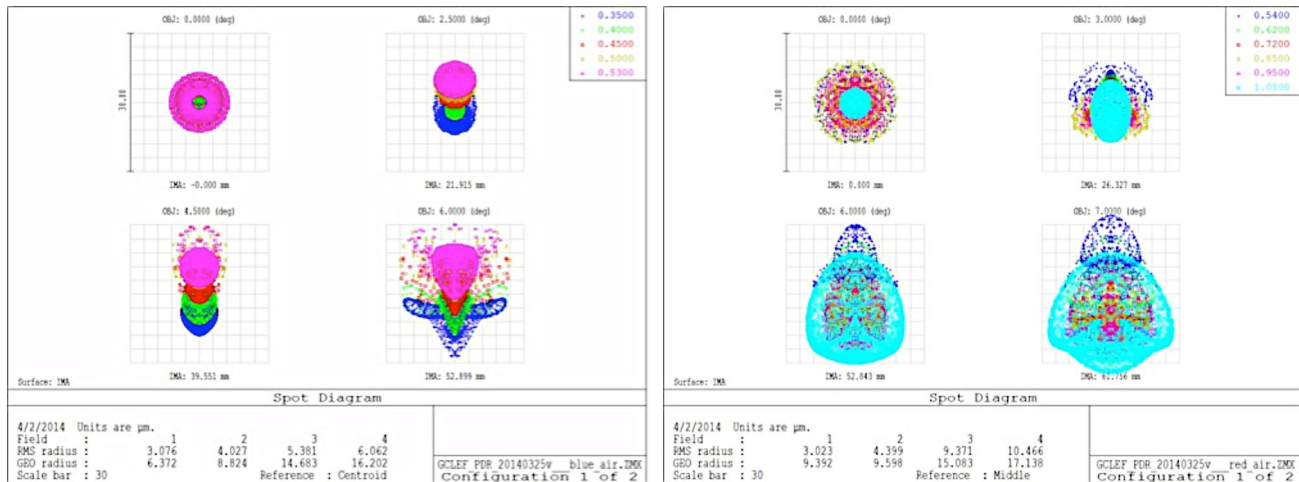


Figure 5 Polychromatic spot diagram for the standalone blue (left) and red (right) cameras in single pass and in air. A modest amount of lateral color is apparent, but nothing to interfere with standalone single-pass testing. Box size is 30x30 microns.

While the cameras have been developed and first optimized in single pass, later in the design process those were re-optimized as part of the vacuum enclosed spectrograph<sup>8</sup>. Therefore the in-air single pass spot diagrams of Figure 5 are not optimal compared to a system that is designed for single-pass imaging only. The figure just illustrates how much of the single pass usability of the camera have been preserved despite the full-spectrograph optimization, and thus how well it can be evaluated as a stand-alone system in air as part of the assembly, integration and test phase.

Ghost image analysis was part of the camera design process and all potential ghost images had been eliminated or softened.

Element	Radius of curv. [mm]	Thickness [mm]	Material	Diameter [mm]
B-L1 front	1199.71	44.34	CaF2	255
B-L1 back	-347.75	19.31		
B-L2 front	-315.56	8.00	BAL35Y	255
B-L2 back	1982.48	2.93		
B-L3 front	374.49	47.05	CaF2	255
B-L3 back	-2585.67	32.93		
B-L4 front	984.41	20.00	PBL1Y	255
B-L4 back	inf.	100.72		
B-L5 front	294.47	51.00	CaF2	230
B-L5 back	-422.81	10.00		
B-L6 front	-378.01	10.00	BSM51Y	220
B-L6 back	218.47	46.44		
B-L7 front	240.28	55.00	CaF2	220
B-L7 back	-616.42	228.13		
<b>refocus for air</b>		0.63		
B-L8 front	209.44	48.00	S-FPL51Y	150
B-L8 back	402.91	18.70		
B-L9 front	-224.06	8.00	BSM51Y	140
B-L9 back	475.94	10.00		

Table 3 Optical prescription of the blue camera

Element	Radius of curv. [mm]	Thickness [mm]	Material	Diameter [mm]
R-L1 front	5400.36	34.00	CaF2	270
R-L1 back	-442.83	16.15		
R-L2 front	-370.78	14.00	BAL35Y	270
R-L2 back	-1490.72	15.15		
R-L3 front	301.29	61.00	CaF2	270
R-L3 back	-660.36	110.99		
R-L4 front	-343.58	20.00	PBM18Y	230
R-L4 back	-891.04	202.60		
R-L5 front	394.53	42.00	CaF2	216
R-L5 back	-523.76	14.72		
R-L6 front	-242.28	12.00	S-LAL12	216
R-L6 back	-564.42	3.72		
R-L7 front	402.51	52.09	CaF2	216
R-L7 back	-324.22	93.53		
refocus for air	0.39			
R-L8 front	-440.05	30.00	S-FPL51Y	150
R-L8 back	896.82	15.76		
R-L9 front	-228.24	8.00	BSM51Y	150
R-L9 back	5996.16	10.00		

Table 4 Optical prescription of the red camera

### 2.3 Operational Modes

The detectors are 6kx6k devices with 15x15 micron pixel size (90x90mm area). The blue camera covers spectral orders 175-114 (3500-5386Å), the red camera records spectral orders 114-61 (5386-10,000Å). The minimum inter-order spacing is 936µm at order 175 in the blue and 896µm at order 114 in the red. These correspond to 3.0 and 2.9 arcseconds on the sky, respectively.

There are 5 modes of operations considered for G-CLEF: two PRV modes, a Medium Resolution (MR), a High Throughput (HT) and a Multi Object Spectroscopy (MOS) mode. For the sake of long term stability the G-CLEF spectrograph optical bench does not employ any active components within the vacuum vessel housing the optics, which might dissipate heat. Therefore the different operating modes are realized by individual fiber feeds, statically mounted very close to each other at the spectrograph slit and each fiber feed equipped with its own focal ratio conversion optics. Observing modes are selected at the front end on the telescope, by injecting light to the desired fiber.

Mode	slit size on sky	angular size of fibers at spectrograph slit	physical size of fiber core [mm]	binning on detector	FWHM in binned pixels	R
PRV	0.79''	0.26'' (7x)	100	1x1	3.65	105 000
MR	0.79''	0.79''	300	3x3	3.68	35 000
HT	1.2''	1.2''	450	5x5	3.28	19 000

Table 5 Summary of G-CLEF fiber feeds (operational modes) and corresponding resolutions. Resolution values are average for red and blue detectors, for the middle of the echellogram. Single detector pixel is 15x15 µm (so 5x5 pixel binning means a 75x75 µm pseudo-pixel).

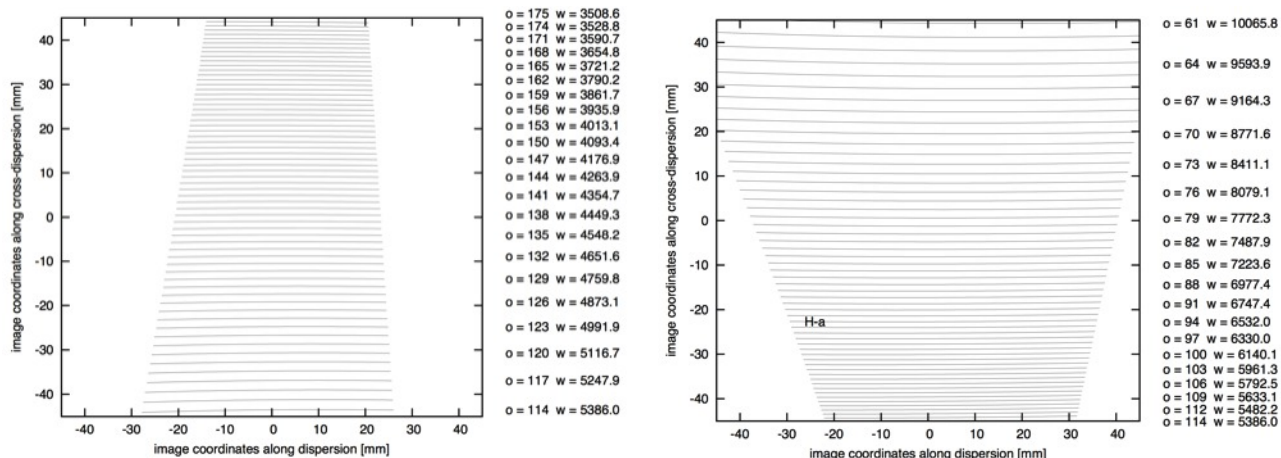


Figure 6 Echellogram format on the blue (left) and red (right) detector

**PRV modes** The unique, segmented primary mirror configuration of the GMT allows for a lossless way of pupil slicing the stellar image by feeding light from each 8.4m primary mirror segment into individual fibers. Thus in the PRV pupil slicer optics the 75 percentile seeing disk of 0.79" is fed into 7 octagonal fibers with a core diameter of 100  $\mu\text{m}$  (f/3 feed). There are two independent PRV fiber feeds. One of the PRV fiber feeds employs an optical double scrambler, while the other trades the increased stability of pupil illumination for higher throughput by not including a scrambler. The spectral resolution is  $R=105\,000$  with an FWHM value of 3.65 pixels using no binning. Since this mode requires the best optical performance it is therefore placed on-axis, at the focus of the collimator mirror. The minimal inter-order spacing allows for clearly distinguished capture of the 7 object fibers plus one sky fiber (see Figure 7). The second PRV fiber feed is identical to the first, except there is no scrambling, which increase throughput.

**MR mode** The Medium Resolution mode feeds the 0.79" seeing disk into a single fiber of 300 $\mu\text{m}$  in size (also at f/3 feed). The spectral resolution is  $R=35,000$  with an FWHM of 3.68 pixels using a 3x3 binning. The echellogram allows for simultaneous recording of an object and a sky fiber.

**HT mode** For fainter stars, a 1.2" sky coverage fiber enables improved throughput but at decreased spectral resolution of 19,000. Sampling of the resolution element is 3.28 pixels using 5x5 binning. Since this mode is the least sensitive to image quality the HT fibers are the farthest (12mm) away from the optical axis, displaced in the dispersion direction. The echellogram allows for simultaneous recording of an object and a sky fiber.

**MOS mode** This mode is essentially identical to the MR mode but hosts a bundle of up to 40 fiber inputs arranged in a pseudo-slit. A different front end, the MANIFEST instrument, feeds these fibers.

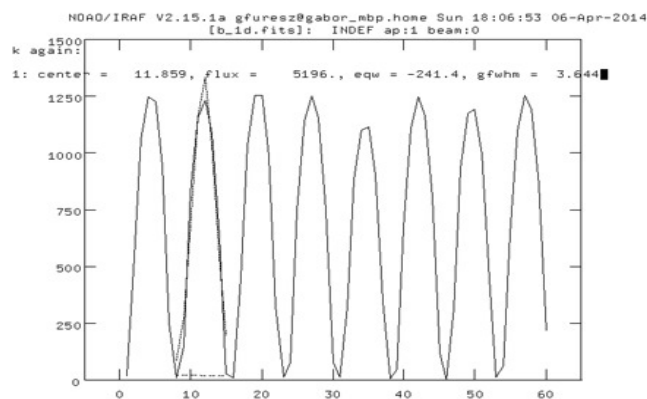


Figure 7 Simulated one-dimensional cross-section (along cross dispersion) of a PRV spectrum. There is a clear separation between the 7 object and 1 sky fiber. Horizontal coordinates are unbinned pixels (1 pixel = 15 microns).

### 3. PERFORMANCE

Figure 8 displays spot diagrams for the PRV mode, following the structure of the echellograms: each spot is placed according to its location on the focal plane. The boxes are 2x2 pixels (30x30 microns), and wavelengths are noted for each box, in Ångströms. The spots are sharp, concentrated, mostly round and smooth. They are also very uniform across a spectral order (horizontally) or at least display a left-to-right symmetry within an order: pots at the short wavelength end of an echelle order are mirrored images of spots seen at the long wavelength end of the same order. This is a result of our design philosophy described in [8].

Figure 8 also shows, for comparison, the size of a PRV fiber on the focal plane at infinite resolution. It is clearly apparent that the pure geometrical image of the fiber end face is much larger than any of the spots, or in other words the PSF of the spectrograph. The shape of the recorded spectral lines, the lines spread function (LSF), is a convolution of this optical transfer function (the PSF) of the spectrograph and the slit input function (the fiber end face). If latter is dominant, then the resulting LSF is uniform across the echellogram and thus the intrinsic spectral line width is not a function of wavelength. If the PSF was dominant (i.e. larger), then the LSF would be driven by the PSF, which is wavelength dependent and therefore the width and shape of spectral lines would be different across the echellogram<sup>8</sup>.

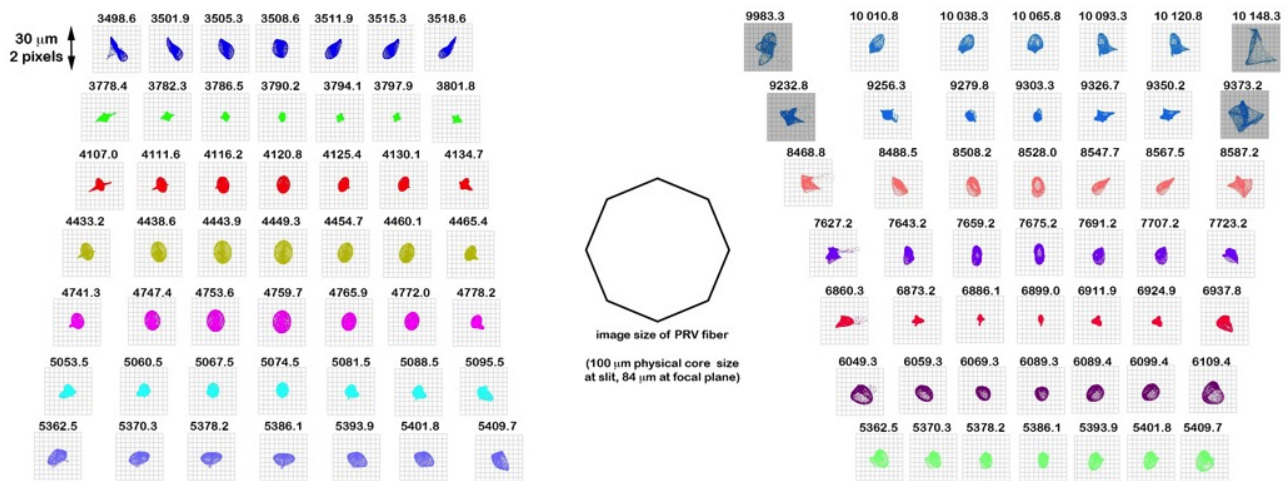


Figure 8 Spot diagrams for the blue (left) and red (right) cameras. See text for details, also refer to Figure 10. Note that the two extreme wavelengths in the reddest two orders fall off the red CCD (thus those boxes are shaded).

Part of the highly successful HARPS approach to PRV measurements was to minimize any variations in the spectrograph environment, since post-facto corrections always leave a certain level of residuals. Our approach was to extend this philosophy to the optical design and make it simple and uniform for data reduction, by providing a highly uniform and simple LSF. Also by design we ensured that changing pupil illumination within the spectrograph, due to imperfect scrambling of the fiber feed, does not affect the shape and position of the LSF and thus induce RV errors. For more details and further discussion please refer to [8].

The as-built systems will always exhibit a more complex LSF due to manufacturing and alignment errors. Therefore we error budgeted these effects on PRV and the tolerancing analysis was very rigorous<sup>5</sup>.

#### 3.1 Spectrograph Efficiency

The predicted efficiency of the spectrograph alone peaks at 37 and 35 % for the blue and the red arms, respectively, and it is mainly shaped by the cross dispersers and the echelle grating. VPH gratings cannot cover too wide of a passband without their efficiency rolling off significantly, and the manufacturer did not provide too optimistic efficiency estimates for the echelle gratings either (<69%). For the mirrors we assumed a multi-layer dielectric coating from Sagem. The blue camera uses highly blue-transmissive glasses, and similarly to the red camera achieves a 76-80% internal transmission, accounting for multi-layer (1-1.5% loss) anti-reflection coatings on each refractive surface.

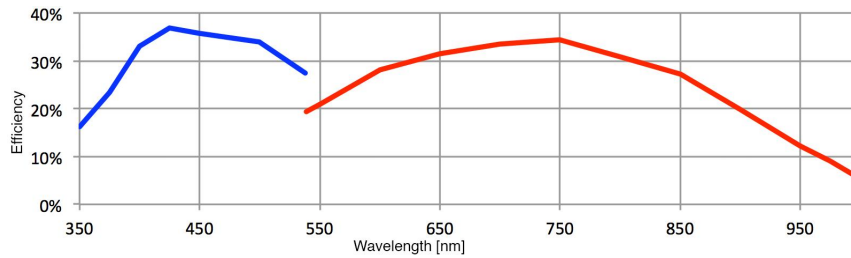


Figure 9 Efficiency estimate for the G-CLEF blue and red arms (spectrograph only, without telescope or fiber run)

#### 4. SUMMARY

We present the optical design of the G-CLEF instrument, a high resolution optical echelle with a PRV capability, being designed for the Giant Magellan Telescope. Since the PRV science case calls for a goal of 0.1m/s precision and comparable level of stability we have considered and incorporated several guidelines in our design philosophy and process that are usually not part of an echelle spectrograph design. At the same time we paid keen attention to keep G-CLEF a generally capable instrument, and thus not to sacrifice other capabilities of the spectrograph (e.g. throughput). As a result we have arrived at a solution that meets the diverse science goals and requirements while employs novel technical solutions, such as the use of a Mangin mirror to correct field curvature. We concluded that to ensure 0.1 m/s RV precision the G-CLEF fiber system need to provide a pupil illumination stability of 0.5% or better, which corresponds to a scrambling gain of  $\sim 8000$ <sup>12</sup>. This can be achieved by using octagonal fibers and an optical double scrambler.

#### REFERENCES

- [1] Szentgyorgyi, A., et al., “The GMT-CfA, Carnegie, Catolica, Chicago Large Earth Finder (G-CLEF): A General Purpose Optical Echelle Spectrograph for the GMT with Precision Radial Velocity Capability”, Proc. SPIE, (2012).
- [2] Bernstein, R., Johns, M., McCarthy, P. Raybould, K., Bigelow, B., Bouchez, A., Filgueira, J., Jacoby, G., Sawyer, D., and Sheehan, M., “Overview and status of the Giant Magellan Telescope”, Proc. SPIE, 9145-47 (These proceedings), (2014)
- [3] A. Baranne, “Equipment Spectrographique du Foyer Coude du Telescope de 3.60 metres,” in ESO CERN Conference on Auxiliary Instrumentation for Large Telescopes, eds. S. Laustsen and A. Reiz, eds., European Southern Observatory-CERN, Geneve, pp. 227–239 (1972)
- [4] Raffaele G. Gratton, Rajiv Bhatia, and Andrea Cavazza “Asymmetric white-pupil collimators for high-resolution spectrographs”, Applied Optics, Vol. 39, Issue 16, pp. 2614-2619 (2000)
- [5] Podgorski, W. A., et al., “A Novel Systems Engineering Approach to the Design of a Precision Radial Velocity Spectrograph - the GMT-Consortium Large Earth Finder (G-CLEF)”, Proc. SPIE, 9147-333 (These proceedings), (2014).
- [6] Mueller, M. et al., “The Opto-Mechanical Design of the GMT-Consortium Large Earth Finder (G-CLEF)”, Proc. SPIE, 9147-347 (These proceedings), (2014)
- [7] Fűrész, G., Zajac, J. and Langellier, N., “Practical aspects of building fiber links for precision radial velocity instruments”, Proc. SPIE, 9151-73 (These proceedings), (2014).
- [8] Fűrész, G. and Epps, H., in prep. for the new SPIE journal JATIS
- [9] Martin, C. et al., “The Keck Cosmic Web Imager”, Proc. SPIE, 77350M (2010)
- [10] Spano, P. et al, “Very high-resolution spectroscopy: the ESPRESSO optical design”, Proc. SPIE 84467V (2010)
- [11] Francesco Pepe, personal communication
- [12] Chazelas, B. et al., “New Scramblers for precision radial velocity : Square and Octagonal fibers.”, Proc. SPIE, 7739-47 (2012)